Solar Polarization 3
ASP Conference Series, Vol. 307, 2003
J. Trujillo Bueno and J. Sánchez Almeida, eds.

IZMIRAN Solar Spectromagnetograph

I. E. Kozhevatov, N. P. Cheragin, E. N. Kulikova

Radiophysical Research Institute, B.Pecherskaya 25, Nizhny Novgorod, 603950 Russia

B. A. Ioshpa, V. N. Obridko, E. A. Rudenchik, and
V. Yu. Nepomnyashchy

Institute of Terrestrial Magnetism, Ionosphere, and Radiowave Propagation, Russian Academy of Sciences, Troitsk, Moscow Reg., 142190 Russia

Abstract.
A new solar spectromagnetograph for measuring the full magnetic-field vector and line-of-sight velocities is described. A new version of a polarization analyzer ensuring parallel measurements of six polarization components of spectral lines is considered. The sensitivity of the instrument for the longitudinal and transverse magnetic field is 5-10 and 30-50 G, respectively, and for the line-of-sight velocities 10 m/s. The procedure of calibration is shortly described.

1. Introduction

There are two main schemes for magnetic fields measurements: a filter–based and spectrograph-based schemes. The first type uses a tunable optical filter, an adjustable polarization analyzer and a two-dimensional CCD array placed in the solar image plane, (Wang et al. 1999, Milkey et al. 1996). The main advantage of this system: data are obtained simultaneously for all points of the image. The disadvantages: the different polarization states are measured sequentially that in conjunction with the time instability of the spectrum device leads to the decreasing of the accuracy of magnetic field determination. In addition, observations are often made only in two spectral regions at line wings. As a result, data can be interpreted only within the framework of the simplest models of the solar atmosphere, which hardly conforms to the reality. Another type of magnetograph scheme uses a diffraction spectrograph with a long entrance slit (Jones et al. 1992, Lites et al. 1993). In this case, the receiving CCD array is located in the spectrum image plane. Such a scheme has a high spectral resolution and ensures simultaneous recording of the intensity over the entire spectrum and along one of the spatial coordinates. However, since the spectrum fluctuations in slit spectrographs are usually higher than those for the filters, this advantage hardly translates into a gain in the accuracy. Nevertheless, the situation can be corrected. As a rule, the maximum number of resolved spectral elements over a line profile is within 20–30. This means that no more than 3-5% of the CCD ar-

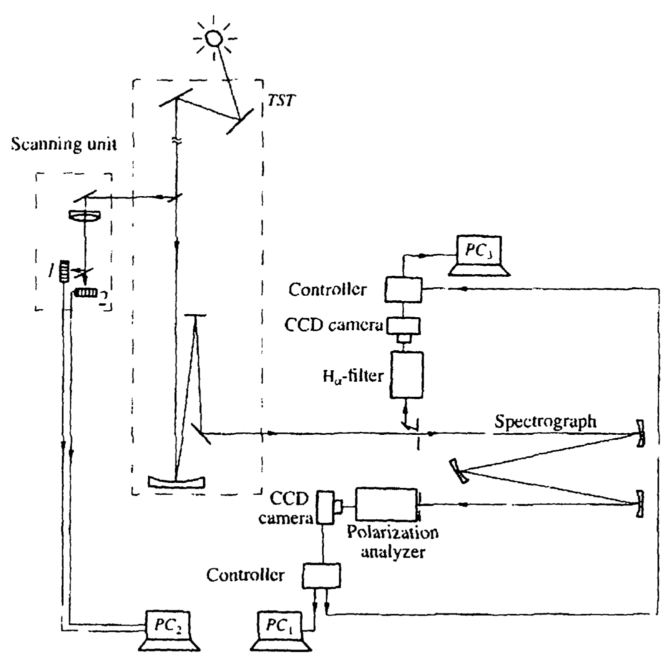

Figure 1. Functional diagram of the spectromagnetograph installed on the TST

ray resolution along one coordinate is used. An obvious conclusion is to design a device for parallel analysis which makes possible to record six polarization components of a spectrum simultaneously. In this case, the time instability of the spectrum loses it's significance because the measurements corresponding to all of the spectrum points are strictly simultaneous for all polarization components. It also reduces the duration of the analysis.

2. General optical layout of the spectromagnetograph

The spectromagnetograph for parallel measurement of the spectral and polarization characteristics of magnetically active lines was designed on the basis of the IZMIRAN solar telescope. Its block diagram is shown in Fig. 1. The general system includes a tower solar telescope (TST), a grating spectrograph, a polarization analyzer, two CCD cameras, two controllers, a scanning unit, an Hα filter and three personal computers (PC). The dispersion of the spectrograph in the second–order spectrum, which is used during the magnetograph's operation, is 0.8 Å/mm. The size of the output slit, which is also the entrance slit of the polarization analyzer, is 20 mm $\times$ 1.5 mm). The CCD cameras (Proscan, Germany) are used in the system as photodetectors. The number of pixels in the CCD array is 1024 $\times$ 1024, and their size is 14 $\times$ 14 μm. The readout rate is 6–10 frame/s. The dark noise and the maximum signal levels correspond to 430 and 16384 units, respectively. The controller ensures signal recording in a digital 16–bit format. A possibility of mutual synchronization of CCD cameras is provided. The TST forms an image of the solar disc 168 mm in diameter on the entrance slit of the spectrograph. The solar radiation transmitted through

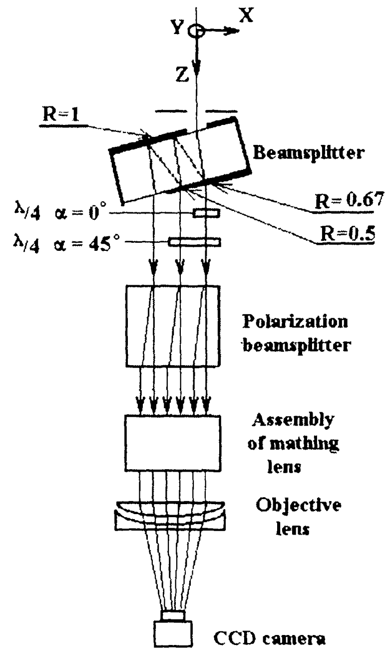

Figure 2. Optical diagram of the parallel–type polarization analyzer

the spectrograph is directed to the polarization analyzer, which forms six bands of the spectrum region corresponding to six polarization states. The intensity of all these bands is recorded by the first CCD camera. Subsequent data is performed with the help of the personal computer PC1. Scanning along one of the spatial coordinates of the active area is carried out by the scanning unit, whose operation is controlled by the second personal computer PC2. The program ensures an absolute referencing of the coordinate system fixed to the guide's photosensors to solar coordinate systems. The solar radiation reflected by the mirror–like jaws of the spectrograph entrance slit passes through the filter used for constructing a solar image in the Hα line. It gives the possibility to have the more precise referencing of the observation data to spatial solar coordinates. The image is read out by the second CCD camera and stored by the third computer PC3.

3. Parallel–type polarization analyzer

Figure 2 shows the optical diagram of such polarization analyzer. The system has a slit, a beam-splitter, two quarter– wavelength plates, a polarization beam splitter, an assembly of matching lenses, and objective lens. The spectrum band with a height of 20 mm and a spectral width of ~1.2 Å is incident on the front plane of the beam-splitter. The spatial beam-splitter is oriented at a 1/8 angle to the optical axis. The first beam passes through two quarter–wavelength plates. The directions of the polarization axes of the first quarter–wavelength plate coincide with the axes of the coordinate system. The directions of the polarization axes of the second $\lambda/4$ plate are turned with respect to those of the first plate clockwise by an angle of 45° in the XY- -plane. The second beam

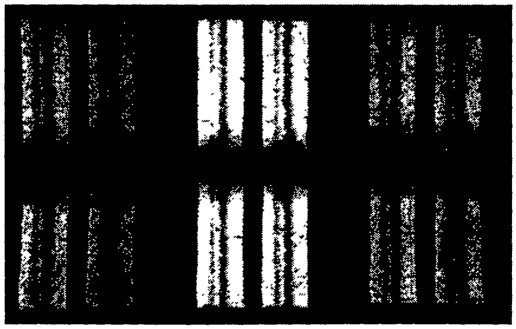

Figure 3. Radiation intensity of the solar spectrum in six different polarizations in the vicinity of the solar spectral line FeI6302.5Å(right) and telluric oxygen line 6302.8Å

passes only the second plate, and the third beam is transmitted unimpeded. Then all three beams fall onto the polarization beam splitter made of the spar where they are transformed into six parallel beams corresponding to different orthogonal linear polarization states and shifted with respect to each other in X–direction. The polarizations of the ordinary and extraordinary waves are directed along the Y and X axes, respectively. With the help of an assembly of mathing lenses and the exit objective lenses three pairs of reduced images are brought to the plane surface of CCD camera. Figure 3 shows the spectrum images in six different polarizations in the vicinity of the FeI solar line λ 6302.5 Å(the Lande factor is 2.5) and the line of atmospheric oxygen λ 6302.8 Å. The latter serves as a reference line in line-of-sight velocity measurements. The radiation corresponds to the cross section of the active region in a sunspot. With the perfectly made quarter–wavelength plates, the intensity values in each of the six beams are described by the expressions

$$J + Q \quad (1) \qquad J - V \quad (4)$$

$$J - Q \quad (2) \qquad J + U \quad (5)$$

$$J + V \quad (3) \qquad J - U \quad (6)$$

Four independent linear equations are sufficient for calculating four parameters. Nevertheless, it is preferable to have these six relations. First, most of the CCD area is not used. On the other hand, the three most important Stokes parameters (Q, V, U) can be easily derived from relations (1)-(6) by appropriate subtractions, making it possible to eliminate any possible additive errors (interferences, noises). This error elimination technique is similar to the modulation method for noise suppression which is widely used in the sequential analysis. In Fig. 4 we give examples of the magnetic maps in the vicinity of the great sunspot obtained on August 27, 2002. The problem of the magnetograph calibration is as important as the development and creation of the optico–electronic system itself. The calibration required to use the interconnected complex of instrumental, mathematical and program facilities. In particular we need

a) determinate the correspondence between the coordinates of the spectrograph entrance slit points and the coordinates of the conjugate with them points

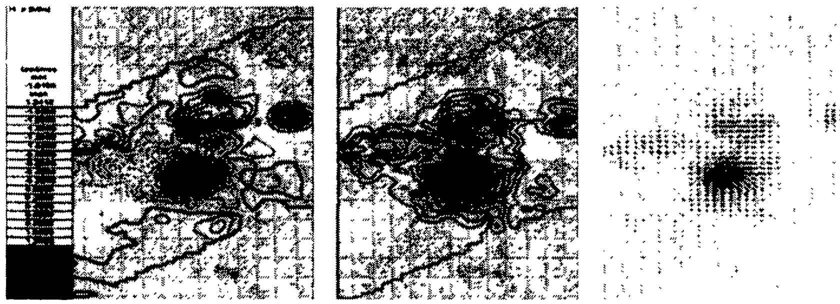

Figure 4. Magnetic field maps for 16.08.02: (a) longitudinal field, (b) transversal field, and (c) azimuthal angle.

of the spectrum of all six parts of CCD–camera corresponding to the different combinations of the polarization optics elements;

b) fix the correspondence between the sensitivities of different CCD–camera pixels;

c) determinate the spatial distribution of the background including the dark current effects of CCD- camera, the influence of the light from the outside sources, the light dispersion on the optical elements etc;

d) account of the effects of defocusing, aberrations, parasitic interference, etc.

4. Conclusions and outlooks

The described spectromagnetograph was mounted on the IZMIRAN tower solar telescope and ensures a sensitivity of 5–10 G in measurements of the longitudinal magnetic field, 30–50 G for the transverse field, ~10 m/s for line-of-sight velocity, permits the use any algorithms for measurements of the magnetic field vector, such as the Babcock algorithm and the Fourier transform method (Ioshpa, Obridko, and Kozhevatov 1996). The described parallel polarization analyzer is entirely static. It contains no controllable elements implying mechanical movements and feeding of electric signals. Therefore, it is much more stable than the mechanical and electro-optical modulators and has almost unlimited life time.

The work was supported by RFBR grant no. 01-02-16357.

References

Ioshpa, B., Obridko, V., & Kozhevatov, I., Solar Phys., 1996, 168, 373

Jones, H.P., Duvall, Th.L., Harvey, J.W., Mahaffey, C., Schwitters, J., & Simmons, J., Solar Phys., 1992, 139, 211

Lites, B.W., Elmore, D.F., Seagraves, P., & Skumanich, A., 1993, ApJ, 418, 928

Milkey, D.L., Canfield, R.C., LaBronte, B.J., Leka, K., Waterson, M., & Weber, H., Solar Phys., 1996, 168, 229

Wang, H., Dencer, C., Spirock, T., Goode, P.R., Yang, S., Marquette, W., Varsic, J., Fear, R., Nenow, J., & Dingley, D., 1999, Solar phys., 183, 1